# A Solid-State Multinuclear Magnetic Resonance Investigation of Hexamethylborazine

**Michelle A. M. Forgeron,[†] David L. Bryce,[†] Roderick E. Wasylishen,*[,†] and Roland Rösler[‡]**

*Department of Chemistry, University of Alberta, Edmonton, Alberta, Canada T6G 2G2, and Department of Chemistry, University of Calgary, Calgary, Alberta, Canada T2N 1N4*

*Received: September 25, 2002*

Analyses of $^{11}$B, $^{13}$C, and $^{2}$H NMR spectra of solid hexamethylborazine, **I**, provide conclusive evidence for rapid in-plane jumps of the borazine ring at room temperature. Boron-11 NMR spectra of magic-angle spinning (MAS) samples, acquired at low (4.7 T), moderate (9.4 T), and high (18.8 T) external applied magnetic field strengths, have been simulated to yield the $^{11}$B nuclear quadrupolar coupling constant ($C_Q$), asymmetry parameter, and isotropic chemical shift; their values at 298 K are 2.98 ± 0.03 MHz, 0.01 ± 0.01, and 36.0 ± 0.4 ppm, respectively. Simulations of $^{13}$C CP/MAS NMR spectra provide the carbon−boron isotropic indirect spin−spin coupling constant, $J_{iso}$, the sign of $C_Q(^{11}B)$, the relative orientations of the boron electric field gradient (EFG) and the $^{13}$C−$^{11}$B dipolar coupling tensors, and the motionally averaged $^{13}$C−$^{11}$B dipolar coupling constant. Variable-temperature $^{2}$H NMR spectra of a partially deuterated sample of **I** indicate that the in-plane jumps of the borazine ring are slow with respect to $C_Q(^2H)^{-1}$ (i.e., $\tau_{jump} \geq 10^{-4}$ s) at temperatures less than 130 K. Over the temperature range 180 to 128 K, $^{2}$H NMR line shape analysis yields an activation energy of 30.1 ± 1.5 kJ mol$^{-1}$ for the in-plane jumps of the borazine ring. Although a precise experimental determination of boron chemical shift anisotropy was impeded by intramolecular and intermolecular boron−boron dipolar interactions and heteronuclear nitrogen−boron dipolar interactions, simulations of high-field $^{11}$B NMR spectra of a stationary sample of **I** suggest a value of 55 ± 15 ppm for the motionally averaged span of the chemical shift tensor. Lastly, high-level ab initio and density functional theory calculations provide values of the boron EFG tensor and the boron and nitrogen magnetic shielding tensors for a rigid molecule of **I**.

## Introduction

Borazines are a class of heterocyclic boron−nitrogen compounds of the general formula $(RBNR')_3$. The parent, borazine (R, R′ = H), which is isoelectronic and isostructural with

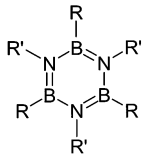

benzene, was discovered in 1926 by Stock and Pohland[1] and has been the subject of considerable theoretical[2−9] and experimental[10−19] interest ever since. Although possessing similar structural and physical properties as the prototypal carbon-based aromatic systems, borazine and its derivatives are chemically much more reactive. Past studies on borazines have focused on their electronic properties,[4−6,9] aromaticity,[8] and their syntheses[20−22] and reactivity.[8,16,22] Several studies on borazines have employed high-resolution multinuclear magnetic resonance spectroscopy in solution;[13,14,17,21] however, relative to benzenes, few solid-state NMR studies have been carried out on the borazine family.[23,24]

Recently, borazine has been successfully used as a precursor for the synthesis of boron nitride,[25] a widely studied ceramic with valuable properties.[26−29] The quality of ceramics has been demonstrated to depend considerably on the architecture of the polymer;[30] hence, the choice of characterization tools is critical for monitoring and controlling polymerization and polymer-to-ceramic conversion. Fazen et al. proposed a route to hexagonal boron nitride (h-BN) by thermal polymerization of borazine to form polyborazylene,[25] a polymer composed of linked borazine rings, followed by pyrolysis under an inert atmosphere, to yield the desired product. This work has been complemented by a characterization study of polyborazylene by Gervais et al. using various $^{11}$B and $^{15}$N solid-state NMR experiments.[28] These NMR techniques proved to be very useful in identifying and differentiating the $^{15}NH_x$ sites ($x = 0-3$) and the two types of boron environments, $BN_2H$ and $BN_3$, in polyborazylene.

In addition to being a powerful tool for characterizing molecular structure, solid-state NMR is a useful technique for probing molecular dynamics.[31−35] Surprisingly, there have been no investigations of molecular motion in solid borazine to date, contrary to the case for solid benzene.[36−41] Similarly, molecular motion occurring in solid hexamethylbenzene has been extensively studied in isolated temperature regions and under various pressure conditions; these data indicate hexad jumps above 150 K and that rapid reorientation of methyl groups persists down to 2 K.[42−47] The present study investigates motion of hexamethylborazine, **I**, in the solid state and characterizes NMR interactions of fundamental interest using various multinuclear ($^{11}$B, $^{13}$C, $^{2}$H, and $^{15}$N) magnetic resonance techniques as well as ab initio and density functional theory (DFT) calculations.

## Theory and Background

**(a) Boron NMR Spectroscopy.** Boron has two naturally occurring isotopes: $^{10}$B and $^{11}$B, both of which possess nuclear

* To whom correspondence should be addressed. Phone: 780-492-4336. Fax: 780-492-8231. E-mail: Roderick.Wasylishen@UAlberta.Ca. Web: http://ramsey.chem.ualberta.ca.

† University of Alberta.

‡ University of Calgary.

10.1021/jp022139x CCC: $25.00 
Published on Web 01/01/2003

magnetic moments. The nuclear spin properties and natural abundances of these isotopes, $^{10}$B ($S = 3$, $\Xi = 10.75$ MHz, $Q = 8.459$ fm$^2$, N.A. = 19.9%) and $^{11}$B ($S = {}^3/_2$, $\Xi = 32.09$ MHz, $Q = 4.059$ fm$^2$, N.A. = 80.1%),[48−50] make them prime candidates for NMR study. In the solid state, the preferred boron NMR isotope is generally boron-11 because the central, $|{}^1/_2\rangle \leftrightarrow \langle -{}^1/_2|$, transition does not depend on the first-order quadrupolar interaction (vide infra).[51−53] The NMR Hamiltonian operator for $^{11}$B nuclei of **I** in the applied magnetic fields, $\mathbf{B}_0$, used in this study is given by

$$\hat{\mathscr{H}} = \hat{\mathscr{H}}_Z + \hat{\mathscr{H}}_{CS} + \hat{\mathscr{H}}_D + \hat{\mathscr{H}}_J + \hat{\mathscr{H}}_Q^{(1)} + \hat{\mathscr{H}}_Q^{(2)} \quad (1)$$

where $\hat{\mathscr{H}}_Z$ represents the Zeeman interaction, $\hat{\mathscr{H}}_{CS}$ represents the nuclear magnetic shielding interaction, $\hat{\mathscr{H}}_D$ and $\hat{\mathscr{H}}_J$ represent the direct dipolar and indirect nuclear spin−spin coupling interactions, respectively, and $\hat{\mathscr{H}}_Q^{(1)}$ and $\hat{\mathscr{H}}_Q^{(2)}$ denote the quadrupolar interaction to first- and second-order, respectively.

**(b) Quadrupolar Interaction.** The quadrupolar interaction results from the interaction of the nuclear quadrupole moment, $eQ$, with the electric field gradient (EFG) at the nucleus. The EFG is described by a symmetric traceless second-rank tensor which, when in its principal axis system (PAS), is diagonal and may be characterized by two independent parameters: the largest principal component, $V_{ZZ} = eq_{ZZ}$, and the asymmetry parameter, $\eta_Q = (V_{XX} - V_{YY})/V_{ZZ}$ with $0 \le \eta_Q \le 1$. The convention used for the magnitudes of the EFG tensor components is such that $|V_{ZZ}| \ge |V_{YY}| \ge |V_{XX}|$ with $V_{ZZ} + V_{YY} + V_{XX} = 0$. To first order, the quadrupolar interaction is given in frequency units by[54]

$$\hat{\mathscr{H}}_Q^{(1)} = \frac{C_Q}{8S(2S-1)}(3\hat{S}_Z^2 - \hat{S}^2)(3\cos^2\theta - 1 + \eta_Q \sin^2\theta \cos 2\phi) \quad (2)$$

where $\theta$ and $\phi$ are polar angles describing the orientation of the EFG tensor with respect to $\mathbf{B}_0$, $\hat{S}$ is the nuclear spin angular momentum operator, and $C_Q$ is the nuclear quadrupole coupling constant, defined in hertz as

$$C_Q = \frac{eQV_{ZZ}}{h} \quad (3)$$

When the quadrupole frequency, $\nu_Q = 3C_Q/[2S(2S-1)]$,[55] is small relative to the Larmor frequency of the quadrupolar nucleus, $\nu_S$, second-order corrections may be made to the energy levels using equations provided by Abragam.[55] Considering only the second-order quadrupolar interaction and assuming $\eta_Q = 0$, these equations indicate that, for $S = {}^3/_2$, the maximum and minimum frequencies of the central, $|{}^1/_2\rangle \leftrightarrow \langle -{}^1/_2|$, transition for a stationary sample are $(\nu_S + C_Q^2/64\nu_S)$ and $(\nu_S - C_Q^2/12\nu_S)$, respectively. From these expressions, it is clear that the breadth of the central transition depends on the inverse of $\nu_S$ (when magnetic shielding anisotropy is neglected) and the square of $C_Q$, thereby making it advantageous to work at the highest possible applied magnetic fields to minimize second-order quadrupolar broadening. In addition to this broadening, the center of gravity of the central transition is shifted away from the true isotropic chemical shift due to second-order quadrupolar effects; for a spin-3/2 nucleus (e.g., $^{11}$B), this shift is given (in hertz) by[56]

$$\nu_{+1/2,-1/2} = -\frac{1}{40}\left(\frac{C_Q^2}{\nu_S}\right)\left(1 + \frac{\eta_Q^2}{3}\right) \quad (4)$$

**(c) Nuclear Magnetic Shielding Interaction.** The nuclear magnetic shielding interaction depends on the orientation of the molecule with respect to $\mathbf{B}_0$ and, thus, may be described by a second-rank tensor, $\boldsymbol{\sigma}$. In isotropic fluids, rapid molecular tumbling averages the shielding tensor to its isotropic value:

$$\sigma_{iso} = (\sigma_{11} + \sigma_{22} + \sigma_{33})/3 \quad (5)$$

which is related to the isotropic chemical shift by

$$\delta_{iso,sample} \approx \sigma_{iso,ref} - \sigma_{iso,sample} \quad (6)$$

In the solid state, the fixed orientation of a molecule allows the symmetric portion of the magnetic shielding tensor to be fully characterized.[57] To accomplish this, one must determine the three principal components of the magnetic shielding tensor and the three angles which define the orientation of the PAS with respect to the molecular axis system. The span, $\Omega$, or breadth of the shielding and chemical shift tensors is described by[58]

$$\Omega = \sigma_{33} - \sigma_{11} = \delta_{11} - \delta_{33} \quad (7)$$

and the line shape by the skew, $\kappa$,[58]

$$\kappa = \frac{3(\sigma_{iso} - \sigma_{22})}{\Omega} = \frac{3(\delta_{22} - \delta_{iso})}{\Omega} \quad (8)$$

which is unitless and can take on values between −1 and +1, inclusive.

**(d) $^2$H NMR Spectroscopy and Molecular Dynamics.** Molecular motion in solids is commonly investigated using $^2$H ($S = 1$) NMR spectroscopy.[31,35,39,59,60] Deuterium NMR spectra are usually completely dominated by the quadrupolar interaction, as the chemical shift anisotropy (CSA) and direct dipolar coupling interactions are relatively small for deuterium.[61,62] The deuterium quadrupolar interaction is well matched to the rate of many dynamic processes in solids;[35] i.e., $C_Q(^2\text{H})$ values are on the order of $10^5$ Hz. Consequently, molecular motions occurring at rates on the order of $10^3$ to $10^7$ Hz may have profound effects on $^2$H NMR line shapes.

In $^2$H NMR studies, the quadrupole echo pulse sequence[63] is often employed as a function of pulse spacing and temperature to provide detailed information about simple motions in solids via dynamic line shape analyses.[35,63,64] It is well-known that in the rigid lattice limit, where all motions are slow with respect to $C_Q(^2\text{H})$, the splitting between the discontinuities of the $^2$H NMR spectrum for an axially symmetric EFG tensor is $3C_Q(^2\text{H})/4$.[35] Thus, if the splitting is known, the quadrupolar coupling constant may be deduced. Noticeable distortions in the line shape accompanied by a dramatic decline in signal intensity indicate that molecular motion is in the intermediate regime, for which the jump or diffusion times are comparable to $C_Q(^2\text{H})^{-1}$ and changes in the line shape are extremely sensitive to small temperature changes. For a planar molecule with $C_3$ or $C_6$ symmetry, when the rate of jumps about the principal symmetry axis is fast with respect to $C_Q(^2\text{H})^{-1}$, the splitting in the $^2$H NMR spectrum is reduced by a factor of $(3\cos^2\beta - 1)/2$, where $\beta$ is the angle between $V_{ZZ}$ and the symmetry axis. In this regime, if the motion has 3-fold or greater symmetry, the line shape will appear axially symmetric and the nature of the motion cannot be distinguished as being small-step diffusion (i.e., continuous motion) or discrete, large-angle jumps.[35]

**(e) Spin-$^1/_2$ Nuclei Dipolar Coupled to Quadrupolar Nuclei.** Significant interest has recently been devoted to the *indirect* study of quadrupolar nuclei by observing neighboring

spin-$^1/_2$ nuclei.[65−67] It is well-known that heteronuclear dipolar interactions between coupled spin-$^1/_2$ nuclei are normally completely removed by the MAS technique; however, when one or both nuclei are quadrupolar, this is not the case.[65−69] For large values of $C_Q$ or at low applied magnetic fields, the high-field approximation breaks down so that the nuclear spin angular momentum of the quadrupolar nuclei is not completely quantized in the direction of the applied field, $\mathbf{B}_0$, but rather there is competition between $\mathbf{B}_0$ and the EFG. Consequently, MAS fails to completely average the dipolar interaction and residual coupling to the quadrupolar nucleus is observed. If the ratio of quadrupolar to Zeeman energies, i.e., $C_Q/[4\nu_S S(2S-1)]$,[70] is small, the resonance frequencies of the quadrupolar nucleus in the MAS NMR spectrum of a spin-$^1/_2$ nucleus coupled to a quadrupolar (spin-$S$) nucleus are given by[71]

$$\nu_m = \nu_L - m|J_{iso}| - \frac{S(S+1) - 3m^2}{S(2S-1)}d \qquad (9)$$

where $m$ is the quantum spin-state of the spin-$S$ nucleus, $\nu_L$ is the Larmor frequency of the spin-$^1/_2$ nucleus, and $d$ is the residual dipolar coupling constant, defined as

$$d = \left(\frac{3C_Q R_{eff}}{20\nu_S}\right)[(3\cos^2\beta^D - 1) + \eta_Q \sin^2\beta^D \cos^2\alpha^D] \qquad (10)$$

Here, $\beta^D$ and $\alpha^D$ are polar angles describing the orientation of the $I-S$ dipolar vector, $r_{IS}$, with respect to the EFG tensor at the spin-$S$ nucleus. Because it is impossible to separate the dipolar coupling and the anisotropy of the $J$-coupling, $\Delta J$,[72] these terms are combined into the *effective* dipolar coupling constant, $R_{eff} = R_{DD} - \Delta J/3$.

From eq 10, it is clear that under favorable conditions, valuable information may be gained from the NMR spectrum of a spin-$I$ nucleus coupled to a spin-$S$ nucleus. First, the isotropic indirect spin−spin coupling constant may be determined, which is generally unavailable from solution NMR due to "self-decoupling", brought on by fast relaxation of the quadrupolar nucleus relative to $J_{iso}$.[73−75] Second, because the NMR line shape of a spin-$I$ nucleus is very sensitive to $C_Q$ and $\eta_Q$ in the presence of residual dipolar coupling under MAS conditions, information about these quadrupolar parameters, as well as the orientation of the EFG tensor, may be gained.

## Experimental and Computational Details

**(a) Preparation of Compounds.** The synthesis of **I** took place in two steps using slightly modified literature procedures.[20] First, *B*-trichloro-*N*-trimethylborazine, $(ClBN(CH_3))_3$ (R = Cl, R′ = $CH_3$), was prepared under an $N_2$ atmosphere by addition of excess $BCl_3$(g) to a slurry of $CH_3NH_3Cl$ in refluxing chlorobenzene. The partially deuterated analogue (R = $CH_3$, R′ = $CD_3$) was synthesized using $CD_3NH_3Cl$, obtained from Aldrich. Formation of the fully methylated product was carried out by reaction of excess $CH_3MgBr$ with $(ClBN(CH_3))_3$ in $Et_2O$, yielding a white crystalline solid. $^1$H and $^{13}$C NMR spectra of **I** in $C_6D_6$(l) were obtained, and the chemical shifts were in excellent agreement with literature values.[20] The melting point of the natural-abundance sample of **I** was found to be 97.1 °C by differential scanning calorimetry (literature value 97−98 °C) and that of the partially deuterated sample was found to be 98.0−98.5 °C. Although the intermediate product is known to be unstable in air, it has been stated that the final product, **I**, is the simplest air-stable derivative of borazine.[20] Despite this claim, impurity peaks became apparent in $^{11}$B, $^{13}$C, and $^{15}$N solid-state NMR spectra when the product was exposed to air for periods of several weeks at room temperature.

**(b) Solid-State NMR Spectroscopy.** Samples of **I** were powdered and packed into 2.5, 4, and 5 mm o.d. zirconia rotors in a nitrogen-filled glovebox. Solid-state $^{11}$B MAS NMR experiments were carried out using Chemagnetics CMX Infinity ($\mathbf{B}_0$ = 4.7 T, $\nu_S(^{11}B)$ = 64.2 MHz), Bruker AMX ($\mathbf{B}_0$ = 9.4 T, $\nu_S(^{11}B)$ = 128.4 MHz) and Varian Inova ($\mathbf{B}_0$ = 17.6 T, $\nu_S(^{11}B)$ = 240.6 MHz and $\mathbf{B}_0$ = 18.8 T, $\nu_S(^{11}B)$ = 256.6 MHz) spectrometers. High-power proton decoupling was used at 4.7, 9.4, and 17.6 T but not at 18.8 T. The magic angle was set by observing the $^{23}$Na NMR free-induction decay and spectrum of solid $NaNO_3$.[31] Referencing and pulse width calibration for $^{11}$B were carried out using solid $NaBH_4$. Boron chemical shifts reported herein are with respect to the boron NMR primary reference, $F_3B{\cdot}O(C_2H_5)_2$(l) at 0.00 ppm. The chemical shift of $NaBH_4$(s) relative to $F_3B{\cdot}O(C_2H_5)_2$(l) is −42.06 ppm.[76] A one-pulse sequence was used to record the boron NMR spectra; pulse widths employed for boron ranged from 0.4 to 5.0 $\mu$s and recycle delays were 0.5 to 10 s. Low-temperature $^{11}$B NMR experiments were also carried out using an automated temperature controller. A pulse-acquire sequence with a selective $\pi/2$ pulse width of 2.5 $\mu$s and a recycle delay of 5 s was used. Acquisition of data commenced at 298 K and the temperature was lowered in increments of 10−30 K until a temperature of 110 K was reached; a minimum stabilization period of 20 min was allotted after each temperature adjustment and the probe tuning was checked prior to acquisition of each spectrum. Due to the well-documented problems associated with measuring sample temperatures with great accuracy,[77−80] temperatures were calibrated using the $^{207}$Pb NMR resonance of a sample of solid $Pb(NO_3)_2$[77−80] according to the method described by van Gorkom et al.[80] The inversion recovery pulse sequence, $[(\pi)_x-\tau-(\pi/2)_x-ACQ]$,[81] was also employed to investigate the spin−lattice relaxation time, $T_1$, of the $^{11}$B nuclei. A recycle delay of 10 s and selective $\pi$ and $\pi/2$ pulse widths of 5.0 and 2.5 $\mu$s, respectively, were used to record 16 scans. Values of $\tau$ varied from 0.001 to 200 ms. The total integrated peak area was calculated to determine the signal intensity for each experiment.

Carbon-13 and deuterium NMR spectra were collected on a Chemagnetics CMX Infinity spectrometer ($\mathbf{B}_0$ = 4.7 T, $\nu_L(^{13}C)$ = 50.3 MHz, $\nu_S(^2H)$ = 30.7 MHz), using high-power proton decoupling for the $^{13}$C NMR spectra. Adamantane was used as a CP/MAS setup sample and secondary reference for $^{13}$C.[32,76,82] A $\pi/2$ proton pulse width of 3.0 $\mu$s, contact time of 12 ms, and a recycle delay of 5 s were used to record 10 240 scans. Variable-temperature deuterium NMR spectra were recorded using the quadrupolar echo pulse sequence $[(\pi/2)_x-\tau_1-(\pi/2)_y-\tau-ACQ]$[63] on a stationary sample of hexamethylborazine-$N_3$-$d_9$ using a Chemagnetics DRNS 5 mm probe. A spectral width of 1 MHz, $\pi/2$ pulse width of 2.0 $\mu$s, acquisition time of 4.096 ms, and pulse delays of 3−12 s were employed. The delays $\tau_1$ and $\tau$ were 21 and 22 $\mu$s, respectively, and data were left-shifted to the top of the echo prior to Fourier transformation. Acquisition of $^2$H NMR spectra commenced at 290 K and temperatures were reduced in 5−20 K increments until a lower limit of 128 K, imposed by the probe, was reached. Sixty-four acquisitions were summed for each temperature, except the spectrum acquired at 128 K, for which 128 scans were acquired. Temperatures were calibrated according to the method described by Beckmann and Dybowski.[78] Although the automated controller reports temperatures to ±0.5 °C, discrepancies in the reported, calibrated temperatures were found to be as large as 12 degrees compared to those given by the temperature controller.

Spectral simulations of $^{11}B$ and $^{13}C$ NMR spectra were carried out using WSOLIDS,[83] a software package developed in this laboratory. This package incorporates the space-tiling algorithm of Alderman et al. for the efficient generation of powder patterns.[84] Deuterium quadrupolar echo spectra were calculated with the program MXQET[85] using a three-site jump model. This program calculates quadrupolar powder patterns for an *n*-site exchange system and accounts for experimental parameters such as the $\pi/2$ pulse length and pulse spacing, $\tau_1$.

**(c) Quantum Chemical Calculations.** Ab initio calculations of the EFG and nuclear magnetic shielding tensors for boron and nitrogen were carried out at the restricted Hartree−Fock (RHF) level of theory using Gaussian 98[86] operating on an IBM RS6000 workstation with dual 200 MHz processors. DFT calculations, using the hybrid Becke three-parameter exchange functional[87] and the Lee−Yang−Parr correlation functional[88] (B3LYP), were also performed. A variety of Pople-type basis sets (6-311G, 6-311+G*, and 6-311++G(3df,3pd)), available from the Gaussian library, were employed. Calculations of nuclear magnetic shielding tensors were carried out using the gauge-including atomic orbitals (GIAO) method.[89] Nuclear quadrupolar coupling constants were calculated using the largest component of the EFG tensor, $V_{ZZ}$ ($=eq_{ZZ}$), and eq 3. The accepted nuclear quadrupole moment, $eQ$, for boron-11 is 4.059 fm$^2$ and that for nitrogen-14 is 2.044 fm$^2$.[90] Conversion of $eq_{ZZ}$ from atomic units to V m$^{-2}$ was carried out using the factor $9.71736 \times 10^{21}$ V m$^{-2}$ per atomic unit.[91] Eigenvalues and direction cosines relating the tensors to the molecular frame were determined by diagonalizing the symmetrized tensors.

Indirect nuclear spin−spin coupling tensors were calculated using the CPL spin−spin coupling module[92] of the Amsterdam density functional (ADF) program[93] running on an IBM RS6000 workstation. The couplings are calculated on the basis of the relativistic zeroth-order regular approximation (ZORA) DFT implementation described in ref 92c,d. ZORA-V Slater-type basis sets available within the ADF package were employed on all atoms and scalar relativistic corrections were accounted for. The Fermi-contact, spin−orbit (paramagnetic and diamagnetic), and spin dipolar mechanisms were included in the calculations.

Because no crystal structure data are available for **I**, the *B*-triethyl-*N*-tripropyl derivative of borazine (R = $C_2H_5$, R′ = $C_3H_7$), whose crystal structure is known,[94] was used in the present calculations to provide the B, N, and $C_{methyl}$ coordinates. Ethyl and propyl groups were replaced by methyl groups with fixed tetrahedral geometries and C−H bond lengths of 1.09 Å;[95] the structure was used without further optimization.

## Results and Discussion

**(a) Boron-11 NMR Spectroscopy.** Boron-11 NMR spectra of the central transition of **I**, shown in Figure 1, have been obtained with MAS at low (4.7 T), moderate (9.4 T), and high (18.8 T) applied magnetic field strengths. The sharp, well-defined $^{11}B$ NMR line shapes are indicative of only one site in the asymmetric unit of solid **I** and are characteristic of line shapes dominated by the second-order quadrupolar interaction. Comparison of the three spectra shown in Figure 1 clearly illustrates the benefits of employing higher magnetic fields. For example, because the breadth of the spectra is proportional to $C_Q^2/\nu_S$, higher magnetic fields result in a decreased splitting between discontinuities; this splitting is reduced from 4089 ± 16 Hz at 4.7 T, to 2075 ± 15 Hz at 9.4 T, to 977 ± 20 Hz at 18.8 T. In addition, the second-order quadrupolar shift, $\nu_{+1/2,-1/2}$, defined in eq 4, decreases with increasing magnetic field from

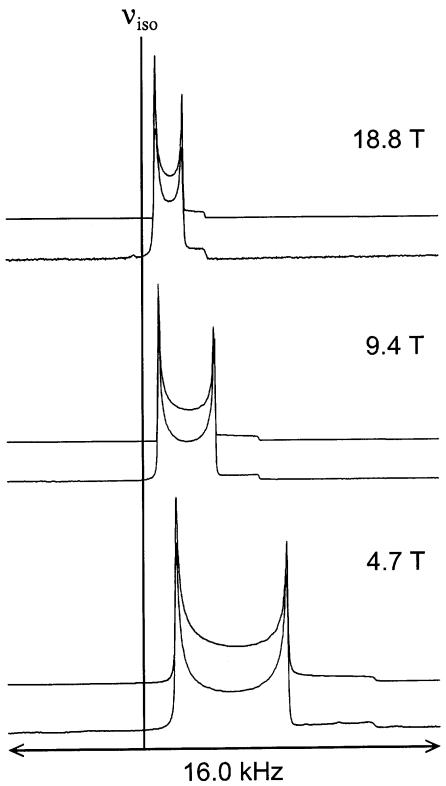


**Figure 1.** Simulated (top) and experimental (bottom) $^{11}B$ NMR spectra of solid **I** at three different applied magnetic fields (4.7, 9.4, and 18.8 T) and MAS rates of 13.0, 25.0, and 8.1 kHz, respectively. The vertical line indicates the isotropic frequency at each applied magnetic field.

**TABLE 1: Comparison of Experimental and Calculated[a] $^{11}B$ NMR Parameters for I**

| | exp (solid state; $T = 298$ K) | calc (isolated, static molecule) |
|---|---|---|
| $C_Q$/MHz | 2.98 ± 0.03 | 3.88 |
| $\eta_Q$ | 0.01 ± 0.01 | 0.14 |
| $\delta_{iso}$/ppm | 36.0 ± 0.4 | |

[a] RHF/6-311++G(3df,3pd). See Experimental Section and ref 94 for structure details.

−53.7 ppm at 4.7 T, to −13.4 ppm at 9.4 T, and to −3.4 ppm at 18.8 T. These splittings and line shapes correspond to values of $C_Q(^{11}B) = 2.98 \pm 0.03$ MHz and $\eta_Q = 0.01 \pm 0.01$ (Table 1). The $^{11}B$ quadrupolar coupling constant may be compared to previously determined values for related compounds. For example, several solid-state $^{11}B$ NMR studies report values of $C_Q(^{11}B)$ ranging from 2.7 to 2.9 MHz for hexagonal boron nitride,[24,31] polyborazylene,[24] and *B*-trialcynylborazine,[24] whereas values of 3.2 and 3.6 MHz have been reported for the parent borazine by nuclear quadrupole resonance (NQR)[15] and solution $^1H$ NMR[13,14] studies, respectively. This range of $^{11}B$ quadrupolar coupling constants is characteristic of $B_3N_3$ ring structures[24] and, in general, values of $C_Q(^{11}B)$ are less than 5 MHz.[96]

Boron and nitrogen NQR[11,12,15] studies of borazine at 77 K report values of $\eta_Q$ that are significantly nonzero at 77 K: $\eta_Q(^{11}B) = 0.133$,[12,15] $\eta_Q(^{14}N) = 0.10$,[15] and $\eta_Q(^{14}N) = 0.097$.[11] The nonzero asymmetry parameters indicate that the borazine ring is not jumping rapidly about its $C_3$ axis at 77 K. Ab initio and DFT calculations for a static molecule of **I** yield nonzero values of $\eta_Q$ (Table 2). In contrast to both the experimental work on borazine[11,12,15] and theoretical calculations, our $^{11}B$ NMR results for **I** indicate that $\eta_Q$ is zero within experimental error at room temperature. This suggests the borazine ring is

**TABLE 2: Experimental and Calculated[a] Boron Nuclear Magnetic Shielding and Quadrupolar Parameters for I**

| | $\sigma_{11}$/ppm | $\sigma_{22}$/ppm | $\sigma_{33}$/ppm | $\sigma_{iso}$/ppm | $\Omega$/ppm | $\kappa$ | $C_Q(^{11}B)$/MHz | $\eta_Q$ |
|---|---|---|---|---|---|---|---|---|
| | | | | Experiment | | | | |
| solid-state $^{11}$B NMR | | | | | $55 \pm 15$ | $1.00 \pm 0.01$ | $2.98 \pm 0.03$ | $0.01 \pm 0.01$ |
| | | | | Calculated | | | | |
| DFT(B3LYP) | | | | | | | | |
| 6-311G | 49.1 | 58.6 | 103.6 | 70.4 | 54.5 | 0.65 | 3.10 | 0.18 |
| 6-311+G* | 43.8 | 55.3 | 100.1 | 66.4 | 56.4 | 0.59 | 3.32 | 0.19 |
| 6-311++G(3df,3pd) | 43.3 | 54.0 | 97.2 | 64.8 | 54.0 | 0.60 | 3.41 | 0.16 |
| RHF | | | | | | | | |
| 6-311G | 63.4 | 71.7 | 113.6 | 82.9 | 50.2 | 0.67 | 3.59 | 0.13 |
| 6-311+G* | 58.8 | 69.9 | 109.5 | 79.4 | 50.7 | 0.56 | 3.79 | 0.16 |
| 6-311++G(3df,3pd) | 57.9 | 68.6 | 107.3 | 78.0 | 49.4 | 0.57 | 3.88 | 0.14 |

[a] Crystal structure data for *B*-triethyl-*N*-tripropylborazine[94] provide values for the B, N, and $C_{methyl}$ coordinates; methyl groups were given fixed tetrahedral geometries with C−H bond lengths of 1.09 Å.

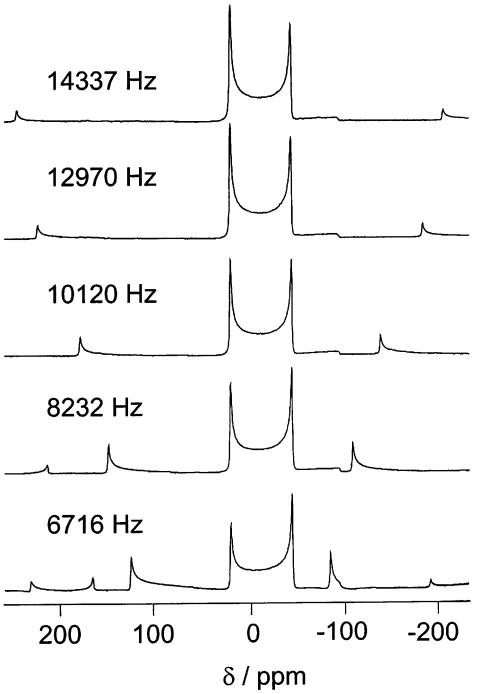


**Figure 2.** Boron-11 NMR spectra of the central transition of MAS samples of solid **I** obtained at 4.7 T for various spinning rates.

jumping rapidly, ($\gg 10^3$ Hz, vide infra), thereby effectively averaging the in-plane components of the EFG tensor. Variable-temperature $^{11}$B NMR experiments indicate that the EFG tensor is axially symmetric within experimental error (i.e., $\eta_Q = 0.03 \pm 0.03$) even at 110 K. Nevertheless, spectral changes were observed in the low-temperature $^{11}$B NMR experiments at 4.7 T. In particular, $C_Q$ increases by approximately 2% at 110 K relative to room temperature, which is likely due to the slowed jumping motion of the borazine ring. To observe a static value of $\eta_Q$, it appears that temperatures much lower than those accessible by our current equipment are required. Furthermore, boron atoms in trigonal environments generally have small values of $\eta_Q$;[14,97] therefore, we expect that the true $\eta_Q$ will be relatively small (i.e., $\eta_Q < 0.2$).

The spectra shown in Figure 2 illustrate the sensitivity of the $^{11}$B central transition line shape to the MAS rate. The relative intensities of the discontinuities of the asymmetric powder pattern change as the spinning rate is changed. A previous literature report[24] on related borazines proposes that distortions in the line shape of $^{11}$B MAS spectra, i.e., the relative intensities of the discontinuities, may be due to coupling of $^{11}$B nuclei with neighboring $^{14}$N quadrupolar nuclei. One may easily estimate the magnitude of this coupling using the direct dipolar coupling constant, $R_{DD}$:

$$R_{DD} = \left(\frac{\mu_0}{4\pi}\right)\left(\frac{\gamma_I \gamma_S \hbar}{2\pi}\right)\langle r_{IS}^{-3}\rangle \qquad (11)$$

For a directly bonded $^{14}$N−$^{11}$B spin-pair, employing a B−N bond length of 1.437 Å from the crystal structure of *B*-triethyl-*N*-tripropylborazine,[94] $R_{DD}(^{14}N,^{11}B)$ is 939 Hz. It may be that residual $^{14}$N, $^{11}$B dipolar coupling contributes to the $^{11}$B NMR spectra obtained by Gervais et al.;[24] however, the use of higher MAS rates or sideband summation with the centerband would likely produce a line shape that matches more closely their simulated spectra.

Our variable-speed MAS NMR data for **I** indicate that $^{14}$N nuclei have a negligible effect on the line shape of the $^{11}$B spectra. If sufficiently high MAS rates are employed, accurate line shapes are obtained and residual dipolar coupling between $^{11}$B and $^{14}$N is not observed. Furthermore, even at an MAS rate as low as 6.7 kHz, summation of sideband intensity into the centerband produces a spectrum that matches the simulated spectrum on the basis of an infinite MAS rate. For **I**, MAS and rapid jumps of the borazine ring combine to effectively average the dipolar interaction (at the fields employed here). In contrast, preliminary $^{11}$B NMR data (not shown) for an MAS sample of *B*-triphenylborazine (R = phenyl; R′ = H) indicate that jumps of the borazine ring are hindered by the bulky phenyl groups; consequently, the full value of $R_{DD}$ is observed for this compound. In the $^{11}$B NMR spectrum of *B*-triphenylborazine obtained with MAS, residual $^{14}$N−$^{11}$B dipolar coupling is clearly observed as a resolved splitting in the discontinuities of the $|^1/_2\rangle \leftrightarrow \langle -^1/_2|$ transition and values of $C_Q$ and $\eta_Q$ are $3.09 \pm 0.03$ MHz and $0.18 \pm 0.04$, respectively. This provides a further example where the lack of molecular motion results in residual dipolar splittings involving two quadrupolar nuclei, first reported by Wu and Yamada for the $^{14}$N−$^{11}$B spin pair in triethanolamine borate,[68] and a nonzero value for $\eta_Q$.

Quantification of the boron CSA in **I** was complicated by intra- and intermolecular $^{11}$B−$^{11}$B and $^{14}$N−$^{11}$B interactions in the stationary sample[97] and also by probe background due to the presence of boron nitride in the stator. However, simulations of $^{11}$B NMR spectra of a stationary sample of **I** at applied magnetic fields of 17.6 and 18.8 T (not shown) provide an estimate of $55 \pm 15$ ppm for the motionally averaged span, with $\kappa = +1.00$ (i.e., axial symmetry).

**(b) Quantum Chemical Calculations.** Ab initio and DFT calculations provide values of the boron and nitrogen nuclear magnetic shielding tensors for a static, isolated molecule of **I** (Table 3). The calculated orientation of these tensors is shown

**TABLE 3: Nuclear Magnetic Shielding Parameters for I,[a] Hexamethylbenzene,[b] and Pyrrole**

| | $\sigma_{11}$/ppm | $\sigma_{22}$/ppm | $\sigma_{33}$/ppm | Ω/ppm | $\kappa$ | $T$/K |
|---|---|---|---|---|---|---|
| Hexamethylborazine (**I**) | | | | | | |
| nitrogen (calc) | 27.9 | 201.5 | 256.0 | 228.1 | 0.52 | |
| boron (calc) | 57.9 | 68.6 | 107.3 | 49.4 | 0.57 | |
| Hexamethylbenzene | | | | | | |
| aryl-carbon (obs)[b] | −6 | −6 | 162 | 168 | 0.00 | 296 |
| aryl-carbon (obs)[b] | −49 | 29 | 159 | 208 | 0.25 | 87 |
| Pyrrole | | | | | | |
| nitrogen (obs)[c] | 0 | 98 | 192 | 192 | −0.02 | 298 |
| nitrogen (calc)[d] | 2 | 104 | 174 | 172 | −0.19 | |

[a] Calculated for **I** using RHF/6-311++(3df,3pd). [b] Determined experimentally by Pines et al. using solid-state $^{13}$C NMR spectroscopy.[37] Carbon-13 chemical shift values, referenced to liquid benzene at 23 °C in ref 37, have been referenced to tetramethylsilane, TMS,[106] and then converted to magnetic shielding values using eq 6 and $\sigma_{iso,TMS}$ (liquid, spherical bulb; 300 K) = 184.1 ppm, determined by Jameson and Jameson.[107] [c] Determined experimentally by Solum et al.[99] using solid-state $^{15}$N NMR spectroscopy. Chemical shift values, referenced to nitromethane at room temperature, have been converted to nitrogen magnetic shielding values using eq 6 and $\sigma_{iso,nitromethane} = -135.8$ ppm).[99] [d] Calculated by Solum et al. using DFT methods.[99]

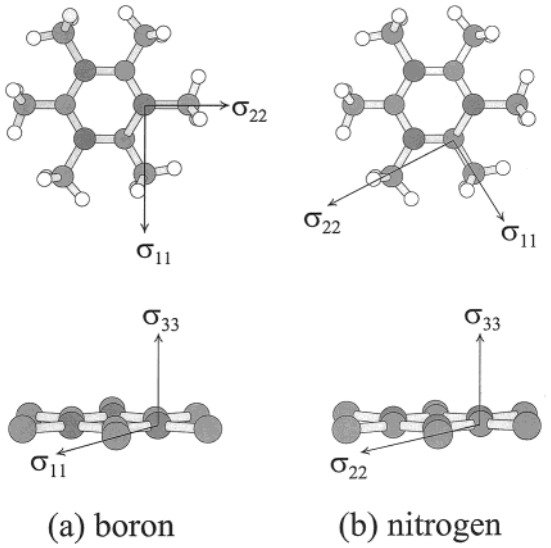


**Figure 3.** Orientation of (a) boron and (b) nitrogen nuclear magnetic shielding tensors in **I**. Components $\sigma_{11}$ and $\sigma_{22}$ lie in the plane of the ring whereas $\sigma_{33}$ is perpendicular to the plane. In the lower figures, the hydrogen atoms have been removed for clarity.

in Figure 3. As inferred from $^{11}$B NMR spectra (vide supra), **I** undergoes rapid in-plane jumps at room temperature, resulting in effective boron and nitrogen magnetic shielding tensors that are axially symmetric due to motional averaging of the in-plane components.

To our knowledge, there are no previous reports of nitrogen or boron magnetic shielding tensors in borazines. In fact, only two experimental reports of boron magnetic shielding tensors have been reported to date.[97,98] Comparison of the calculated shielding tensors in **I** may therefore be made to those of analogous three-coordinate systems. Here we compare the *aryl*-carbon magnetic shielding tensor in hexamethylbenzene[37] and the nitrogen magnetic shielding tensor in pyrrole[99] to the calculated boron and nitrogen magnetic shielding tensors in **I**, respectively. This comparison is reasonable because the systems under consideration are planar with similar electronic structures; thus the orientation of their shielding tensors, which is dictated by the local molecular symmetry, is expected to be similar. For example, in aromatic systems, the most shielded component is

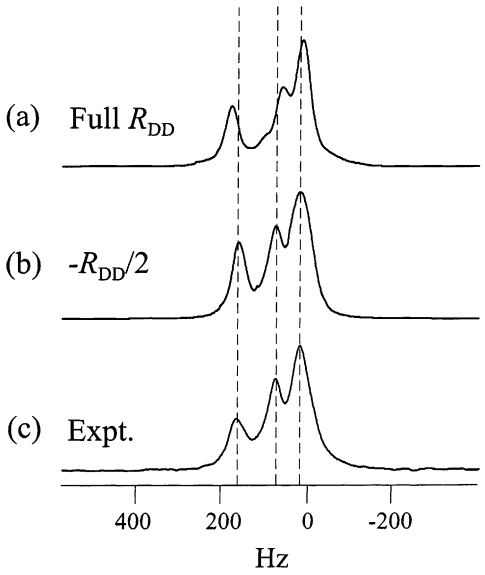


**Figure 4.** Simulated $^{13}$C CP/MAS NMR spectra of solid **I** at 4.7 T considering (a) the full value of $R_{DD}(^{13}C,^{11}B)$, 2403 Hz, and (b) the motionally averaged value, $-R_{DD}(^{13}C,^{11}B)/2 = -1202$ Hz. The simulated spectra account for *both* $^{10}$B and $^{11}$B coupling to carbon in the weighted ratio of their natural abundances to fit (c) the experimental spectrum ($\nu_{rot} = 6.18$ kHz).

perpendicular to the molecular plane, one component must be along a $C_2$ axis in the molecular plane, and the third must be in the plane, perpendicular to the first two components. The calculated principal components of the boron and nitrogen magnetic shielding tensors in **I**, along with literature results for the carbon and nitrogen shielding tensors in hexamethylbenzene and pyrrole, are summarized in Table 3. For hexamethylbenzene,[37] the experimental carbon NMR line shape is axially symmetric at room temperature, but asymmetric at 87 K due to slowed motion of the benzene ring.[37] A summary of the tensor orientations, depicted in Figure 3, is as follows: the component in the direction of greatest shielding, $\sigma_{33}$, is oriented perpendicular to the ring in all cases. For nitrogen in **I**, the intermediate shielding component, $\sigma_{22}$, is tangential to the borazine ring whereas the component in the direction of least shielding, $\sigma_{11}$, is along the internuclear N−C vector. On the other hand, for boron in **I**, $\sigma_{22}$ is along the internuclear B−C vector, whereas $\sigma_{11}$ is tangential to the borazine ring. The orientations of the *aryl*-carbon and nitrogen magnetic shielding tensor for hexamethylbenzene and pyrrole are analogous to the nitrogen and boron shielding tensors in **I**, respectively.

**(c) Carbon-13 CP/MAS NMR Spectroscopy.** In the $^{13}$C NMR spectrum of an MAS sample of **I**, two distinct peaks are evident, one for each type of methyl carbon (i.e., B−C and N−C). First, we focus on the signal due to the methyl carbons that are directly bonded to boron which shows splittings due to residual dipolar coupling to both $^{10}$B and $^{11}$B.[65−67] Shown in Figure 4c is an expansion of the experimental $^{13}$C CP/MAS NMR spectrum (4.7 T) of **I**, (R = $CH_3$, R′ = $CD_3$), showing only the peaks that arise from those carbon atoms bonded to boron. The simulated spectra are also shown in Figure 4 and the values of the best-fit parameters (Figure 4b) are listed in Table 4. The best-fit simulated spectrum (Figure 4b) incorporates the assumption of rapid in-plane jumps of the borazine ring and also the residual heteronuclear spin−spin interactions between $^{13}$C and *both* boron isotopes in the ratio of their natural abundances. The best-fit simulated spectrum indicates that $J(^{13}C,^{11}B) = 57 \pm 2$ Hz (Table 4), which is within the range one would expect for $^1J(^{13}C,^{11}B)$.[100] ZORA-DFT calculations

**TABLE 4: $^{13}$C NMR Parameters Obtained from MAS Samples of I at 4.7 T[a]**

| $\delta_{iso}$/ppm | $J_{iso}(^{13}C,^{11}B)$/Hz | $C_Q(^{11}B)$/MHz | $R_{DD}(^{13}C,^{11}B)$/Hz | $d$/Hz |
|---|---|---|---|---|
| $1.0 \pm 0.1$ | $57 \pm 2$ | $2.98 \pm 0.03$ | $-1202 \pm 100$ | 22.28 |

[a] The indirect spin−spin and dipolar coupling values for $^{13}$C,$^{10}$B can be determined from the ratio of the magnetogyric ratios for $^{10}$B and $^{11}$B, and the quadrupolar coupling constant for $^{10}$B from the ratio of their quadrupole moments. Their values are as follows: $J_{iso}(^{13}C,^{10}B) = 19$ Hz, $R_{DD}(^{13}C,^{10}B) = 401$ Hz, and $C_Q(^{10}B) = 6.20$ MHz. From the simulations, the sign of $C_Q(^{11}B)$ is found to be positive and the magnitude of $C_Q(^{11}B)$, first obtained from $^{11}$B spectra, is confirmed.

carried out on a static molecule of **I** predict values for $J(^{13}C,^{11}B)$ and $\Delta J(^{13}C,^{11}B)$ of 50.1 and 22.6 Hz, respectively. The calculated value for $J_{iso}(^{13}C,^{11}B)$ is in excellent agreement with both solid-state and solution experimental values and, from the calculated value of $\Delta J(^{13}C,^{11}B)$, it is clear that $\Delta J/3$ (=7.5 Hz) is negligible compared to $R_{DD}(^{13}C,^{11}B) = 2403$ Hz ($r_{CB} = 1.592$ Å).[94]

In fitting the $^{13}$C CP/MAS NMR spectrum, rapid jumps of the borazine ring about the principal $C_3$ axis were assumed. In the absence of rapid jumps, the largest component of the dipolar tensor, $-2R_{DD}$, lies along the internuclear B−C vector; however, rapid jumps about the $C_3$ axis average the in-plane components of the dipolar tensor, $-2R_{DD}$ and $R_{DD}$, thereby reducing the component along the B−C vector to $-R_{DD}/2$. Note that the largest component of the reduced $^{11}$B−$^{13}$C dipolar coupling tensor is now perpendicular to the borazine ring and collinear with $V_{ZZ}(^{11}B)$; thus $\beta^D$ in eq 10 is 0°. Use of the reduced dipolar coupling constant, $-R_{DD}(^{13}C,^{11}B)/2 = -1202$ Hz, gave a spectral simulation that is in very good agreement with the experimental spectrum (Figure 4b) whereas use of the full, unaveraged $^{13}$C, $^{11}$B dipolar coupling constant, 2403 Hz, resulted in an unacceptable fit (Figure 4a). Notice that the best-fit spectrum (Figure 4b) does not perfectly match the experimental spectrum. In particular, the intensities of the high-frequency side of the observed and calculated spectra are unequal; there is an apparent broadening in the experimental spectrum that cannot be reproduced in the simulated spectra. Recent $^{31}$P NMR studies of cobaloximes[101] indicate that the NMR spectrum of an $I = {}^1/_2$ nucleus that is spin-coupled to a quadrupolar (spin-$S$) nucleus may exhibit unexpected line shapes when $T_1(S)^{-1}$ is on the same order of magnitude as $^1J(I,S)$.[73] These distortions are manifested as broadened peaks rather than the expected, well-resolved multiplet structure.[101] Investigation of the relaxation times of $^{11}$B nuclei in **I** using the inversion recovery experiment reveals that the apparent $T_1(^{11}B)$ for the central transition is $80 \pm 20$ ms. Furthermore, the appearance of the simulated $^{13}$C MAS spectra depends strongly on $^1J(^{13}C,\ ^{11}B)$ (=$57 \pm 2$ Hz; Table 4). It is therefore reasonable to conclude that, because the relaxation rate of the boron nuclei is the same order of magnitude as the indirect spin−spin coupling interaction between $^{13}$C and $^{11}$B, discrepancies between the experimental and calculated spectra are likely due to the onset of self-decoupling of the boron nuclei.

The carbon nuclei directly bonded to nitrogen give rise to a single peak in the $^{13}$C CP/MAS NMR spectrum with an isotropic chemical shift of 34.4 ppm and a line width at half-height of $79 \pm 3$ Hz, showing no apparent fine structure due to coupling with $^{14}$N at 4.7 T. The calculated, nonaveraged value of $R_{DD}(^{14}N,^{13}C)$ for $^{14}$N−$^{13}$C ($r_{NC} = 1.475$ Å)[94] is 680 Hz. When motion of the borazine ring is considered, this value is reduced to −340 Hz. Using a calculated (RHF/6-311++G(3df,3pd)) $C_Q(^{14}N)$ value of 2.62 MHz, $R_{DD}(^{14}N,^{13}C) = -340$ Hz, and assuming that $\Delta J = 0$, a residual dipolar coupling constant, $d$, of −18.5 Hz is obtained. Hence, given that $d$ is small and the value of $^1J(^{14}N,^{13}C)$ is probably less than 5 Hz,[102,103] it is not surprising that $^{14}$N−$^{13}$C splittings are not observed in the $^{13}$C CP/MAS NMR spectrum.

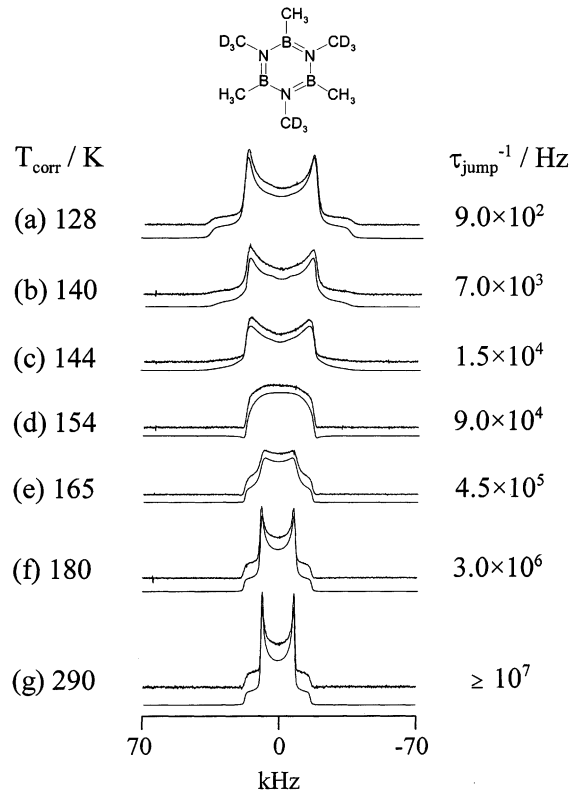


**Figure 5.** Experimental and simulated $^2$H NMR spectra of a stationary sample of partially deuterated **I** at 4.7 T as a function of temperature. The calculated line shapes incorporate a three-site jump model of the borazine ring, infinitely fast methyl group jumps, and an *effective* $^2$H quadrupolar coupling constant of $46 \pm 1$ kHz. For a static molecule of **I**, $C_Q(^2H)$ is 165 kHz. The calibrated temperatures, $T_{corr}$, and jump rates of the borazine ring, $\tau_{jump}^{-1}$, are given.

**(d) Variable-Temperature Deuterium NMR Spectroscopy.** Variable-temperature $^2$H NMR spectra of stationary samples of partially deuterated **I**, (R = $CH_3$, R′ = $CD_3$) are shown in Figure 5 and provide additional conclusive evidence of rapid in-plane jumps of the borazine ring at temperatures as low as 170 K. At room temperature, there are two types of motion taking place simultaneously: rapid jumps of the borazine ring about the principal $C_3$ axis (or pseudo-$C_6$ axis) and rapid jumps of the methyl groups about their local $C_3$ axes. Together, these motions reduce the splitting between the discontinuities in the $^2$H NMR spectra for a static molecule of **I** by their respective scaling factors: $(3\cos^2\beta - 1)/2$, where $\beta$ is defined as the angle between $V_{ZZ}$ and the axis of rotation (i.e., ideally $\beta = 90°$ and 109.47° for jumps of the borazine ring and the methyl groups, respectively). Fast jumps of the borazine ring should therefore decrease the separation between discontinuities by a factor of 2, whereas rapid jumps of the methyl groups should decrease the splitting by a factor of 3.

The $^2$H NMR spectrum acquired at 290 K (Figure 5) is indicative of axial symmetry of the $^2$H EFG with a splitting between discontinuities of $23 \pm 1$ kHz, which is in excellent agreement with the value of 22.7 kHz reported for hexamethylbenzene.[58] As a rough approximation, one can determine the separation between peaks in the absence of motion using the term, $3C_Q(^2H)/4$. For a stationary methyl group, $C_Q(^2H)$ is approximately 165 kHz;[58] thus, the splitting between peaks for

a static molecule of **I** is predicted to be 124 kHz. Because the dynamics described above are expected to reduce this separation to (124/6) kHz, i.e., 21 kHz, the 23 kHz splitting observed at room temperature supports our interpretation.

The lack of change in the appearance of the spectra from 290 to 173 K indicates that jumps of the borazine ring are in the fast-motion regime; i.e., they are fast with respect to $C_Q(^2H)^{-1}$. A three-site jump model used in fitting the variable-temperature spectra provides a jump rate on the order of $10^7$ Hz; however, a six-site jump model was also tested and gave identical results. At approximately 180 K there is a slight decrease in signal intensity relative to the $^2H$ powder pattern at room-temperature accompanied by a distinct change in the $^2H$ NMR line shape, both of which indicate that the ring jumps are now in the intermediate-motion regime. In this region, the $^2H$ NMR line shape is extremely sensitive to subtle temperature changes, resulting in severe distortions and changes in the $^2H$ NMR line shapes compared to typical $^2H$ powder patterns (with $\eta_Q = 0.00$) when the rate of motion is in the fast- or slow-motion limit. These distortions, which become more conspicuous at 154 K, are due to the slowed motion of the borazine ring with respect to $C_Q(^2H)^{-1}$ and to the $T_2$ anisotropy in the sample, which gives rise to an irreversible signal decay that cannot be refocused by the second $\pi/2$ pulse.[35] Lower limit temperature spectra at 140 and 128 K suggest that the borazine ring jumps are now near the slow-motion regime by the re-appearance of a Pake-like doublet, now at twice the separation at 290 K. This doubling of the quadrupolar splitting from 23 ± 1 kHz at 290 K to 46 ± 2 kHz at 128 K confirms that the ring jumps are now slow with respect to $C_Q(^2H)^{-1}$. The splitting of 46 ± 2 kHz for **I** is close to the splitting of 52 kHz obtained for hexamethylbenzene[44] when jumps of the benzene ring are in the slow-motion regime. The larger splitting in the spectrum for hexamethylbenzene may be caused by differences in the $C_{aryl}-C_{methyl}-D$ bond angle in hexamethylbenzene relative to the $N-C_{methyl}-D$ bond angle in **I**, differences in the values of $C_Q(^2H)$ for $C-CD_3$ compared to $N-CD_3$, or may be due to the freezing out of additional motions in hexamethylbenzene, such as lattice vibrations and molecular oscillations.[42]

From the scaling factor of the peak splitting, $(3\cos^2\beta - 1)/2$, it is clear that the motion of the methyl groups is not frozen out by the decrease in temperature because slowed motion of the methyl groups would increase the separation of the splitting in the $^2H$ NMR spectrum by a further factor of 3. In addition, because jumps of the methyl groups in solid hexamethylbenzene are known to have a low activation energy, $E_a = 7.9 \pm 0.4$ kJ mol$^{-1}$,[42] motion of the methyl groups in **I** are expected to persist well below 128 K. In the slow-motion limit of methyl group jumps, a Pake-like doublet with a splitting of 138 kHz is expected: a factor of 3 larger than the splitting observed at 128 K.

An Arrhenius plot of the jump rates as a function of temperature provides the activation energy for jumps of the borazine ring about its $C_3$ or pseudo-$C_6$ axis. Note that, from the $^2H$ NMR line shapes, one cannot determine whether the mechanism for the in-plane motion of the borazine ring in **I** proceeds by small-step diffusion, $C_3$ jumps, or $C_6$ jumps; however, given the packing constraints in a solid, we prefer a jump model. Using the rates which are most sensitive to changes in temperature (i.e., 128−180 K), $E_a$ is determined to be 30.1 ± 1.5 kJ mol$^{-1}$. This value is somewhat higher than that found for hexamethylbenzene-$d_{18}$, 22.2 ± 0.8 kJ mol$^{-1}$, also using $^2H$ NMR line shape analyses.[44] This increase in the activation energy for **I** relative to hexamethylbenzene is reasonable given that the symmetry of the borazine ring ($C_3$ or pseudo-$C_6$) is reduced compared to the perfect $C_6$ symmetry of the benzene ring.[42]

**(e) Nitrogen-15 NMR Spectroscopy.** Nitrogen-15 NMR spectra of MAS and static samples of hexamethylborazine-$^{15}N_3$ obtained at 4.7 T provide $\delta_{iso}(^{15}N)$ and qualitative information about the span of the nitrogen magnetic shielding tensor. With respect to $NH_3(l)$, $\delta_{iso}(^{15}N)$ for solid **I** is 104.6 ppm, which is in excellent agreement with $\delta_{iso}(^{15}N) = 102.9$ ppm, for hexamethylborazine-$^{15}N_3$ dissolved in $CH_2Cl_2$.[104] The presence of few spinning sidebands at an MAS rate of 2.5 kHz renders difficult the measurement of the span as 200 ± 50 ppm using the Herzfeld-Berger[105] method. This procedure, however, is not strictly valid due to the presence of two quadrupolar nuclei ($^{10/11}B$) that are directly bonded to nitrogen. The value of the motionally averaged span obtained from ab initio calculations (RHF/6-311++(3df,3pd)) on **I** is 141 ppm whereas, for a static molecule, $\Omega = 228$ ppm. The value of the span for a static molecule of **I** is within experimental error of both the calculated, 172 ppm, and observed, 192 ppm, values for nitrogen in pyrrole.[99]

## Conclusions

This work provides an interesting example of how multinuclear magnetic resonance techniques provide valuable insights into the molecular structure and dynamics of solids. In particular, in the absence of diffraction data, our solid-state NMR results indicate that there is one unique molecule in the asymmetric unit of **I**. Dynamic line shape analyses of variable-temperature $^2H$ NMR spectra provide conclusive evidence of motion of the borazine ring about its $C_3$ (or pseudo-$C_6$) axis and indicate that jumps of the borazine ring are rapid with respect to $C_Q(^2H)$ at temperatures as low as 180 K whereas jumps of the methyl groups are fast even at 128 K. An Arrhenius plot indicates that the activation energy for jumps of the borazine ring about its $C_3$ axis is 30.1 ± 1.5 kJ mol$^{-1}$. Multifield $^{11}B$ NMR studies illustrate the importance of higher magnetic fields to reduce second-order quadrupole broadening and increase the precision of the quadrupolar coupling parameters. Residual dipolar coupling in the $^{13}C$ CP/MAS NMR spectrum is taken advantage of to confirm the $^{11}B$ quadrupole parameters and the orientations of the $^{11}B$ EFG and carbon−boron spin−spin interaction tensors. Ab initio and DFT calculations provide insight into the boron and nitrogen nuclear magnetic shielding tensors and their orientation with respect to the molecular frame, indicating that the largest component, $\sigma_{33}$, is perpendicular to the ring for both nuclei.

**Acknowledgment.** We thank Dr. Klaus Eichele at the University of Tübingen and members of the solid-state NMR group at the University of Alberta for helpful discussions. Prof. Glenn Penner and Andrea McCullough at the University of Guelph are thanked for discussions on $^2H$ NMR simulations. We are grateful to Prof. Neil Burford at Dalhousie University for use of his lab in preparing initial samples and to Prof. T. Stanley Cameron for his attempts in obtaining a crystal structure of **I**. High-field (18.8 T) spectra were obtained at the Environmental Molecular Sciences Laboratory (a national scientific user facility sponsored by the U.S. DOE Office of Biological and Environmental Research) located at Pacific Northwest National Laboratory, operated by Battelle for the DOE. We thank NSERC for research grants. D.L.B. thanks NSERC, Dalhousie University, the Izaak Walton Killam Trust, and the Walter C. Sumner Foundation for post-graduate scholarships. M.A.M.F. thanks

NSERC, the Alberta Ingenuity Fund, and the University of Alberta for post-graduate scholarships. R.E.W. is a Canada Research Chair in Physical Chemistry and thanks NSERC and the University of Alberta for funding.

## References and Notes

(1) Stock, A.; Pohland, E. *Ber. Deutsch. Chem. Ges.* **1926**, *59*, 2215−2223.
(2) Suzuki, M.; Kubo, R. *Mol. Phys.* **1963**, *7*, 201−209.
(3) Bock, H.; Fuss, W. *Angew. Chem., Int. Ed. Engl.* **1971**, *10*, 182−183.
(4) Blustin, P. H. *Mol. Phys.* **1978**, *36*, 279−285.
(5) Boyd, R. J.; Choi, S. C.; Hale, C. C. *Chem. Phys. Lett.* **1984**, *112*, 136−141.
(6) Armstrong, D. R.; Clark, D. T. *Theor. Chim. Acta* (*Ber.*) **1972**, *24*, 307−316.
(7) Nelson, J. T.; Pietro, W. J. *Inorg. Chem.* **1989**, *28*, 544−548.
(8) Kiran, B.; Phukan, A. K.; Jemmis, E. D. *Inorg. Chem.* **2001**, *40*, 3615−3618.
(9) Vasudevan, K.; Grein, F. *Theor. Chim. Acta* (*Ber.*) **1979**, *52*, 219−229.
(10) Doering, J. P.; Gedanken, A.; Hitchcock, A. P.; Fischer, P.; Moore, J.; Olthoff, J. K.; Tossell, J.; Raghavachari, K.; Robin, M. B. *J. Am. Chem. Soc.* **1986**, *108*, 3602−3608.
(11) Lötz, A.; Voitländer, A.; Smith, J. A. S.; Hyna, V.; Nöth, H. *Chem. Phys.* **1986**, *103*, 317−323.
(12) Lötz, A.; Voitländer, J. *J. Magn. Reson.* **1983**, *54*, 427−435.
(13) Whitesides, G. M.; Regen, S. L.; Lisle, J. B.; Mays, R. *J. Phys. Chem.* **1972**, *76*, 2871−2877.
(14) Mellon, E. K.; Coker, B. M.; Dillon, P. B. *Inorg. Chem.* **1972**, *11*, 852−857.
(15) Lötz, A.; Voitländer, J.; Smith, J. A. S. *Z. Naturforsch. A* **1986**, *41*, 206−207.
(16) Chiavarino, B.; Crestoni, M. E.; Fornarini, S. *J. Am. Chem. Soc.* **1999**, *121*, 2619−2620.
(17) Ito, K.; Watanabe, H.; Kubo, M. *J. Chem. Phys.* **1961**, *34*, 1043−1049.
(18) Steinberg, H.; Brotherton, R. J. *Organoboron Chemistry*; Wiley: New York, 1966; Vol. II.
(19) Maringgele, W. *The Chemistry of Inorganic Homo- and Heterocycles*; Academic: New York, 1987; Vol. I, Chapter 2.
(20) (a) Ryschkewitsch, G. E.; Harris, J. J.; Sisler, H. H. *J. Am. Chem. Soc.* **1958**, *80*, 4515−4517. (b) Haworth, D. T.; Hohnstedt, L. F. *J. Am. Chem. Soc.* **1960**, *82*, 3860−3862.
(21) Framery, E.; Vaultier, M. *Heteroatom Chem.* **2000**, *11*, 218−225.
(22) Paine, R. T.; Koestle, W.; Borek, T. T.; Wood, G. L.; Pruss, E. A.; Duesler, E. N.; Hiskey, M. A. *Inorg. Chem.* **1999**, *38*, 3738−3743.
(23) Marian, C. M.; Gastreich, M. *Solid State Nucl. Magn. Reson.* **2001**, *19*, 29−44.
(24) Gervais, C.; Babonneau, F.; Maquet, J.; Bonhomme, C.; Massiot, D.; Framery, E.; Vaultier, M. *Magn. Reson. Chem.* **1998**, *36*, 407−414.
(25) Fazen, P. J.; Remsen, E. E.; Beck, J. S.; Carroll, P. J.; McGhie, A. R.; Sneddon, L. G. *Chem. Mater.* **1995**, *7*, 1942−1956.
(26) Paine, R. T.; Narula, C. K. *Chem. Rev.* **1990**, *90*, 73−91.
(27) Gastreich, M.; Marian, C. M. *J. Comput. Chem.* **1998**, *19*, 716−725.
(28) Gervais, C.; Maquet, J.; Babonneau, F.; Duriez, C.; Framery, E.; Vaultier, M.; Florian, P.; Massiot, D. *Chem. Mater.* **2001**, *13*, 1700−1707.
(29) Bastow, T. J.; Massiot, D.; Coutures, J. P. *Solid State Nucl. Magn. Reson.* **1998**, *10*, 241−245.
(30) (a) Laine, R. M.; Babonneau, F. *Chem. Mater.* **1993**, *5*, 260−279. (b) Birot, M.; Pillot, J. P.; Dunogues, J. *Chem. Rev.* **1995**, *95*, 1443−1477.
(31) Bryce, D. L.; Bernard, G. M.; Gee, M.; Lumsden, M. D.; Eichele, K.; Wasylishen, R. E. *Can. J. Anal. Sci. Spectrosc.* **2001**, *46*, 46−82.
(32) Schmidt-Rohr, K.; Spiess, H. W. *Multidimensional Solid-State NMR and Polymers*; Academic Press: London, 1994.
(33) Duer, M. J. In *Solid-State NMR Spectroscopy*: *Principles and Applications*, Duer, M. J., Ed.; Blackwell Science: Oxford, U.K., 2002; Vol. 1, Chapter 6.
(34) Brown, S. P.; Spiess, H. W. *Chem. Rev.* **2001**, *101*, 4125−4155.
(35) Griffin, R. G.; Beshah, K.; Ebelhäuser, R.; Huang, T. H.; Olejniczak, E. T.; Rice, D. M.; Siminovitch, D. J.; Wittebort, R. J. In *The Time Domain in Surface and Structural Dynamics*, Long, G. J., Grandjean, F., Eds.; Kluwer Academic Publishers: Boston, 1988; Chapter 7.
(36) Andrew, E. R.; Eades, R. G. *Proc. R. Soc. A* **1953**, *218*, 537.
(37) Pines, A.; Gibby, M. G.; Waugh, J. S. *Chem. Phys. Lett.* **1972**, *15*, 373−376.
(38) Ok, J. H.; Vold, R. R.; Vold, R. L.; Etter, M. C. *J. Phys. Chem.* **1989**, *93*, 7618−7624.
(39) Boden, N.; Clark, L. D.; Hanlon, S. M.; Mortimer, M. *Faraday Symp.* **1978**, *13*, 109−123.
(40) Linder, M.; Höhener, A.; Ernst, R. R. *J. Magn. Reson.* **1979**, *35*, 379−386.
(41) Strub, H.; Beeler, A. J.; Grant, D. M.; Michl, J.; Cutts, P. W.; Zilm, K. W. *J. Am. Chem. Soc.* **1983**, *105*, 3333−3334.
(42) Allen, P. S.; Cowking, A. *J. Chem. Phys.* **1967**, *47*, 4286−4289.
(43) Takeshita, H.; Suzuki, Y.; Nibu, Y.; Shimada, H.; Shimada, R. *Bull. Chem. Soc. Jpn.* **1999**, *72*, 381−387.
(44) Schwartz, L. J.; Meirovitch, E.; Ripmeester, J. A.; Freed, J. H. *J. Phys. Chem.* **1983**, *87*, 4453−4461.
(45) Fyfe, C. A. *Solid State NMR for Chemists*; C. F. C. Press: Ontario, 1983.
(46) Rothwell, W. P.; Waugh, J. S. *J. Chem. Phys.* **1981**, *74*, 2721−2732.
(47) Ackerman, J. L.; Eckman, R.; Pines, A. *Chem. Phys.* **1979**, *42*, 423−428.
(48) Harris, R. K. *Nuclear Magnetic Resonance Spectroscopy*, Longman House: Harlow, 1986.
(49) Harris, R. K.; Becker, E. D.; Cabral de Menezes, S. M.; Goodfellow, R.; Granger, P. In *Encyclopedia of Nuclear Magnetic Resonance*; Grant, D. M., Harris, R. K., Eds.; John Wiley & Sons: New York, 1996; Vol. 9, pp 5−19.
(50) (a) Sundholm, D.; Olsen, J. *J. Chem. Phys.* **1991**, *94*, 5051−5055. (b) Pyykkö, P. *Z. Naturforsch. A* **1992**, *47*, 189−196.
(51) Freude, D.; Haase, J. In *NMR, Basic Principles and Progress*; Diehl, P., Fluck, E., Günther, H., Kosfeld, R., Seelig, J., Eds.; Springer-Verlag: Berlin, 1993; Vol. 29, pp 1−90.
(52) Amoureux, J. P.; Fernandez, C.; Granger, P. In *Multinuclear Magnetic Resonance in Liquids and Solids − Chemical Applications*; Granger, P., Harris, R. K., Eds.; Kluwer Academic Publishers: Dordrecht, The Netherlands, 1990; pp 409−424.
(53) Taulelle, F. In *Multinuclear Magnetic Resonance in Liquids and Solids − Chemical Applications*; Granger, P., Harris, R. K., Eds.; Kluwer Academic Publishers: Dordrecht, The Netherlands, 1990; pp 393−407.
(54) Duer, M. J. In *Solid-State NMR Spectroscopy*: *Principles and Applications*, Duer, M. J., Ed.; Blackwell Science: Oxford, U.K., 2002; Vol. 1, Chapter 1.
(55) Abragam, A. *Principles of Nuclear Magnetism*, Adair, R. K., Elliott, R. J., Marshall, W. C., Wilkinson, D. H., Eds.; Clarendon Press: Oxford, 1961.
(56) Samoson, A. *Chem. Phys. Lett.* **1985**, *119*, 29−32.
(57) (a) Haeberlen, U. In *Advances in Magnetic Resonance*, Waugh, J. S., Ed.; Academic Press: New York, 1976; Suppl. 1, Chapter VI. (b) Anet, F. A. L.; O'Leary, D. J. *Concepts Magn. Reson.* **1991**, *3*, 193-214.
(58) Mason, J. *Solid State Nucl. Magn. Reson.* **1993**, *2*, 285−288.
(59) Hoatson, G. L.; Vold, R. L. In *NMR Basic Principles and Progress*, Diehl, P., Fluck, E., Günther, H., Kosfeld, R., Seelig, J., Eds.; Springer-Verlag: Berlin, 1994; Vol. 32, Chapter 67.
(60) Schmidt-Rohr, K.; Spiess, H. W. *Multidimensional Solid-State NMR and Polymers*; Academic Press: London, 1994.
(61) Vega, A. J. In *Encyclopedia of Nuclear Magnetic Resonance*, Grant, D. M., Harris, R. K., Eds.; Wiley: Chichester, U.K., 1996; pp 3869−3889.
(62) Freude, D.; Haase, J. In *NMR, Basic Principles and Progress*; Diehl, P., Fluck, E., Günther, H., Kosfeld, R., Seelig, J., Eds.; Springer-Verlag: Berlin, 1996; Vol. 34, pp 3−26.
(63) Davis, J. H.; Jeffrey, K. R.; Bloom, M.; Valic, M. I.; Higgs, T. P. *Chem. Phys. Lett.* **1976**, *42*, 390−394.
(64) Sternin, E.; Bloom, M.; MacKay, A. L. *J. Magn. Reson.* **1983**, *55*, 274−282.
(65) Harris, R. K.; Olivieri, A. C. *Prog. Nucl. Magn. Reson. Spectrosc.* **1992**, *24*, 435−456.
(66) (a) Harris, R. K. In *Encyclopedia of Nuclear Magnetic Resonance*; Grant, D. M., Harris, R. K., Eds.; Wiley: Chichester, U.K., 1996; pp 2909−2914. (b) McDowell, C. A. In *Encyclopedia of Nuclear Magnetic Resonance*; Grant, D. M., Harris, R. K., Eds.; Wiley: Chichester, U.K., 1996; pp 2901−2908.
(67) Grondona, P.; Olivieri, A. C. *Concepts Magn. Reson.* **1993**, *5*, 319−339.
(68) Wu, G.; Yamada, K. *Chem. Phys. Lett.* **1999**, *313*, 519−524.
(69) Wi, S.; Frydman, V.; Frydman, L. *J. Chem. Phys.* **2001**, *114*, 8511−8519.
(70) Olivieri, A. C. *Solid State Nucl. Magn. Reson.* **1992**, *1*, 345−353.
(71) Olivieri, A. C. *J. Magn. Reson.* **1989**, *81*, 201−205.
(72) (a) Wasylishen, R. E. In *Encyclopedia of Nuclear Magnetic Resonance*, Grant, D. M., Harris, R. K., Eds.; Wiley: Chichester, U.K., 1996; pp 1685−1695; (b) Wasylishen, R. E. In *Encyclopedia of Nuclear Magnetic Resonance*, Grant, D. M., Harris, R. K., Eds.; Wiley: Chichester, U.K., 2002; pp 274−282.
(73) (a) Hoelger, C.-G.; Rössler, E.; Wehrle, B.; Aguilar-Parrilla, F.; Limbach, H.-H. *J. Phys. Chem.* **1995**, *99*, 14271−14276. (b) Spiess, H. W.; Haeberlen, U.; Zimmermann, H. *J. Magn. Reson.* **1977**, *25*, 55−66. (c) Olivieri, A. C. *J. Chem. Soc., Perkin Trans. 2* **1990**, 85−89. (d) Alarcón, S. H.; Olivieri, A. C.; Jonsen, P. *J. Chem. Soc., Perkin Trans. 2* **1993**, 1783−1786.

(74) Sanders, J. C. P.; Schrobilgen, G. J. In *Multinuclear Magnetic Resonance in Liquids and Solids−Chemical Applications*; Granger, P., Harris, R. K., Eds.; Kluwer: Dordrecht, The Netherlands, 1990; Vol. 322, pp 157−186.

(75) Mlynarik, V. *Prog. Nucl. Magn. Reson. Spectrosc.* **1986**, *18*, 277−305.

(76) Hayashi, S.; Hayamizu, K. *Bull. Chem. Soc. Jpn.* **1989**, *62*, 2429−2430.

(77) Mildner, T.; Ernst, H.; Freude, D. *Solid State Nucl. Magn. Reson.* **1995**, *5*, 269−271.

(78) Beckmann, P. A.; Dybowski, C. *J. Magn. Reson.* **2000**, *146*, 379−380.

(79) $^{207}$Pb chemical shifts in the $^{207}$Pb NMR spectra of $Pb(NO_3)_2$ are extremely sensitive to changes in temperature. Temperature calibrations should always be carried out when variable-temperature NMR experiments are conducted.

(80) van Gorkom, L. C. M.; Hook, J. M.; Logan, M.; Hanna, J. V.; Wasylishen, R. E. *Magn. Reson. Chem.* **1995**, *33*, 791−795.

(81) Farrar, T. C.; Becker, E. D. *Pulse and Fourier Transform NMR: Introduction to Theory and Methods*; Academic: New York, 1971.

(82) (a) Hayashi, S.; Hayamizu, K. *Bull. Chem. Soc. Jpn.* **1991**, *64*, 685−687. (b) Earl, W. L.; VanderHart, D. L. *J. Magn. Reson.* **1982**, *48*, 35−54.

(83) Eichele, K.; Wasylishen, R. E. *WSOLIDS NMR Simulation Package*. 2000, Version 1.17.26.

(84) Alderman, D. W.; Solum, M. S.; Grant, D. M. *J. Chem. Phys.* **1986**, *84*, 3717−3725.

(85) Greenfield, M. S.; Ronemus, A. D.; Vold, R. L.; Vold, R. R.; Ellis, P. D.; Raidy, T. E. *J. Magn. Reson.* **1987**, *72*, 89−107.

(86) Frisch, M. J.; Trucks, G. W.; Schlegel, H. B.; Scuseria, G. E.; Robb, M. A.; Cheeseman, J. R.; Zakrzewski, V. G.; Montgomery, J. A., Jr.; Stratmann, R. E.; Burant, J. C.; Dapprich, S.; Millam, J. M.; Daniels, A. D.; Kudin, K. N.; Strain, M. C.; Farkas, O.; Tomasi, J.; Barone, V.; Cossi, M.; Cammi, R.; Mennucci, B.; Pomelli, C.; Adamo, C.; Clifford, S.; Ochterski, J.; Petersson, G. A.; Ayala, P. Y.; Cui, Q.; Morokuma, K.; Malick, D. K.; Rabuck, A. D.; Raghavachari, K.; Foresman, J. B.; Cioslowski, J.; Ortiz, J. V.; Stefanov, B. B.; Liu, G.; Liashenko, A.; Piskorz, P.; Komaromi, I.; Gomperts, R.; Martin, R. L.; Fox, D. J.; Keith, T.; Al-Laham, M. A.; Peng, C. Y.; Nanayakkara, A.; Gonzalez, C.; Challacombe, M.; Gill, P. M. W.; Johnson, B.; Chen, W.; Wong, M. W.; Andres, J. L.; Gonzalez, C.; Head-Gordon, M.; Replogle, E. S.; Pople, J. A. Gaussian 98, Revision A.4; Gaussian, Inc.: Pittsburgh, PA, 1998.

(87) Becke, A. D. *J. Chem. Phys.* **1993**, *98*, 5648−5652.

(88) Lee, C. T..; Yang, W. T.; Parr, R. G. *Phys. Rev. B.* **1988**, *37*, 785−789.

(89) (a) Ditchfield, R. *Mol. Phys.* **1974**, *27*, 789. (b) Wolinski, K.; Hinton, J. F.; Pulay, P. *J. Am. Chem. Soc.* **1990**, *112*, 8251−8260.

(90) (a) Neyens, G.; Coulier, N.; Teughels, S.; Georgiev, G.; Brown, B. A.; Rogers, W. F.; Balabanski, D. L.; Coussement, R.; Lépine-Szily, A.; Lewitowicz, M.; Mittig, W.; de Oliveira Santos, F.; Roussel-Chomaz, P.; Ternier, S.; Vyvey, K.; Cortina-Gil, D. *Phys. Rev. Lett.* **1999**, *82*, 497−500. (b) Minamisono, T.; Ohtsubo, T.; Sato, K.; Takeda, S.; Fukuda, S.; Izumikawa, T.; Tanigaki, M.; Miyake, T.; Yamaguchi, T.; Nakamura, N.; Tanji, H.; Matsuta, K.; Fukuda, M.; Nojiri, Y. *Phys. Lett. B*. **1998**, *420*, 31−36. (c) Pyykkö, P. *Mol. Phys.* **2001**, *99*, 1617−1629.

(91) Mills, I.; Cvitaš, T.; Homann, K.; Kallay, N.; Kuchitsu, K. *Quantities, Units and Symbols in Physical Chemistry*, 2nd ed.; Blackwell Science: Oxford, U.K., 1993.

(92) (a) Dickson, R. M.; Ziegler, T. *J. Phys. Chem.* **1996**, *100*, 5286−5290. (b) Khandogin, J.; Ziegler, T. *Spectrochim. Acta* **1999**, *A55*, 607−624. (c) Autschbach, J.; Ziegler, T. *J. Chem. Phys.* **2000**, *113*, 936−947. (d) Autschbach, J.; Ziegler, T. *J. Chem. Phys.* **2000**, *113*, 9410−9418.

(93) (a) ADF 2000.01, Theoretical Chemistry, Vrije Universiteit, Amsterdam, http://www.scm.com. (b) Baerends, E. J.; Ellis, D. E.; Ros, P. *Chem. Phys.* **1973**, *2*, 41−51. (c) Versluis, L.; Ziegler, T. *J. Chem. Phys.* **1988**, *88*, 322−328. (d) te Velde, G.; Baerends, E. J. *J. Comput. Phys.* **1992**, *99*, 84−98. (e) Fonseca Guerra, C.; Snijders, J. G.; te Velde, G.; Baerends, E. J. *Theor. Chem. Acc.* **1998**, *99*, 391−403.

(94) Boese, R.; Bläser, D.; Stellberg, P.; Maulitz, A. H. *Z. Kristallogr.* **1995**, *210*, 638−639.

(95) Jeffrey, G. A.; Ruble, J. R.; McMullan, R. K.; Pople, J. A. *Proc. R. Soc. London A* **1987**, *414*, 47−57.

(96) Bailey, W. C. *J. Magn. Reson.* **1997**, *185*, 403−407.

(97) Bryce, D. L.; Wasylishen, R. E.; Gee, M. *J. Phys. Chem. A* **2001**, *105*, 3633−3640.

(98) Kroeker, S.; Stebbins, J. F. *Inorg. Chem.* **2001**, *40*, 6239−6246.

(99) Solum, M. S.; Altmann, K. L.; Strohmeier, M.; Berges, D. A.; Zhang, Y. L.; Facelli, J. C.; Pugmire R. J.; Grant, D. M. *J. Am. Chem. Soc.* **1997**, *119*, 9804−9809.

(100) Wrackmeyer, B. In *Annual Reports on NMR Spectroscopy*; Webb, G. A., Ed.; Academic: London, 1988; Vol. 20, p 61.

(101) Schurko, R. W.; Wasylishen, R. E. *J. Phys. Chem. A* **2000**, *104*, 3410−3420.

(102) Eichele, K.; Wasylishen, R. E. *Solid State Nucl. Magn. Reson.* **1992**, *1*, 159−163.

(103) Witanowski, M.; Stefaniak, L.; Webb, G. A. In *Annual Reports on NMR Spectroscopy*; Webb, G. A., Ed.; Academic: London, 1986; Vol. 18, p 1.

(104) Witanowski, M.; Stefaniak, L.; Webb, G. A. In *Annual Reports on NMR Spectroscopy*; Webb, G. A., Ed.; Academic: London, 1981; Vol. 11, p 221.

(105) Herzfeld, J.; Berger, A. E. *J. Chem. Phys.* **1980**, *73*, 6021−6030.

(106) Duncan, T. M. *Principal Components of Chemical Shift Tensors*: *A Compilation*, 2nd ed.; Farragut Press: Chicago, 1994.

(107) (a) Jameson, A. K.; Jameson, C. J. *Chem. Phys. Lett.* **1987**, *134*, 461−466. (b) Jameson, C. J. In *Encyclopedia of Nuclear Magnetic Resonance*, Grant, D. M., Harris, R. K., Eds.; Wiley: Chichester, U.K., 1996; pp 1273−1281. (c) An alternative $^{13}$C magnetic shielding scale has been proposed: Raynes, W. T.; McVay, R.; Wright, S. J. *J. Chem. Soc., Faraday Trans. 2* **1989**, *85*, 759−763.